Full Paper

Journal of the Brazilian Chemical Society

https://dx.doi.org/10.21577/0103-5053.20260051

J. Braz. Chem. Soc. **2026**, *37*, e-20260051, 1-11

Combined Cloud Point and Magnetic Solid-Phase Extraction Using Magnetized *Moringa oleifera* for Cadmium Determination in Aqueous Samples

Deborah C. B. Gonçalves, [a] ***James M. Silva,*** [a] ***Weida R. Silva*** [a] ***and Vanessa N. Alves*** *,[a]

[a]*Instituto de Química, Universidade Federal de Catalão (UFCAT), 75704-020 Catalão-GO, Brazil*

Cadmium contamination in aquatic environments poses significant environmental and health risks, reinforcing the need for sensitive and selective analytical approaches. Traditional sample preparation techniques often fall short in selectivity and sensitivity, motivating the development of alternative strategies. This study introduces a novel hybrid method that combines cloud point extraction (CPE) with magnetic solid-phase extraction (MSPE) for the efficient extraction of cadmium ions from aqueous samples. *Moringa oleifera* shells, modified with a ferromagnetic fluid, were employed as an eco-friendly and low-cost magnetic adsorbent and fully characterized. Key parameters such as extraction pH and adsorbent mass were optimized, establishing pH 6 and 20.0 mg. A 2^4 factorial design identified optimal extraction conditions with 1% Triton X-100, 1.0 mol L^{-1} HNO_3, 5 min sonication, and 6 min heating. Selectivity was assessed via a fractional factorial design involving seven metal ions, revealing no interference from Co^{II}, Fe^{III}, Mn^{II}, and Ni^{II}. The method demonstrated good analytical performance, with a sensitivity of 1.8×10^{-3}, linear range of 0.25-2000.0 μg L^{-1}, limit of detection (LOD) of 3.45 μg L^{-1}, limit of quantification (LOQ) of 11.5 μg L^{-1}, and precision values of 7.71% (overall), 5.12% (repeatability), and 2.56% (reproducibility).

Keywords: cadmium, SPE, adsorbent alternatives, environmental monitoring

Introduction

Population growth and the expansion of industrial, livestock, and agricultural activities have intensified the release of metal ions into the environment. These contaminants are commonly found in packaging, water, agricultural products, cosmetics, and food. And are of particular concern due to their persistence, non-biodegradable nature, and ability to bioaccumulate, posing risks to both human health and ecosystems.[1-3] Their toxicity is influenced by factors such as concentration, exposure time, route of exposure, and chemical speciation.[4,5]

Unlike organic pollutants, metal ions can persist in the environment for long periods, during which they undergo geochemical transformations that can increase their toxicity through bioaccumulation and biomagnification along the food chain.[6,7] In humans, exposure may lead to cumulative effects.[8-10] Cadmium (Cd), for instance, is well known for its nephrotoxic effects and its tendency to accumulate in the kidneys and liver.[11-14] Since food and drinking water represent the main exposure pathways,[15] the development of reliable monitoring and remediation strategies is essential to minimize environmental and public health impacts.[5] Therefore, the accurate determination of metal ions is crucial for maintaining quality of life.[1,2,15,16]

Spectroscopic techniques are widely employed for the determination of metals in environmental samples. Advances in analytical methodologies are continuously required to improve detection and quantification limits.[17,18] Commonly used techniques include flame atomic absorption spectrometry (FAAS),[19] graphite furnace atomic absorption spectrometry (GFAAS),[20] inductively coupled plasma optical emission spectrometry (ICP-OES),[21,22] and inductively coupled plasma mass spectrometry (ICP-MS).[23,24] Despite their adequate sensitivity and selectivity, these techniques strongly depend on efficient sample preparation. This step is essential to reduce matrix effects, enable analyte preconcentration, and improve detection limits. Consequently, the development of simple, efficient, and environmentally friendly sample preparation strategies is fundamental for the determination of toxic metals, such as cadmium, in complex environmental matrices.[25-27]

*e-mail: vanessa.nunes@ufcat.edu.br
Editor handled this article: César Ricardo Teixeira Tarley (Associate)

Sample preparation is a crucial step in trace metal analysis, as it removes interfering species, concentrates the analyte, and enhances detection limits. Among various methods, solid-phase extraction (SPE) has been widely used due to its simplicity, low cost, and versatility with different types of adsorbents. Although not a new technique, SPE has been enhanced and innovated to meet current needs for more advanced and environmentally friendly sample preparation methods, supporting green chemistry without compromising the analytical quality of the method. In this context, natural adsorbents have emerged as sustainable alternatives to traditional solid phases, as they are abundant, renewable, and contain functional groups capable of binding with metal ions.[28-30] Recently, *Moringa oleifera* has attracted particular attention among natural adsorbents due to its versatility and effectiveness in various extraction methods for metal ions.[31,32] While many studies highlight its use as a natural coagulant, more recent research emphasizes its promising ability to adsorb and remove various compounds, including metal ions.[33-35] The surface of these materials can be modified during cleaning with acidic or basic solutions, and they can also be altered by saturation with magnetic fluids, which impart magnetic properties.

Modifying *Moringa oleifera* shells with magnetic fluids creates a magnetized adsorbent that improves microextraction techniques.[33] Adding magnetic properties to this natural material enables its use in magnetic solid-phase extraction (MSPE), a type of solid-phase extraction that eliminates the need for centrifugation and filtration steps.[36,37] In this method, the analyte-loaded adsorbent can be rapidly and effectively separated from water using an external magnetic field, simplifying the extraction process, reducing analysis time, and supporting more environmentally friendly analytical methods.[38,39] These chemical and physical modifications enhance their usefulness, with magnetic modification being especially advantageous because it simplifies phase separation and increases operational efficiency. MSPE is often used in environmental monitoring, particularly for the removal and detection of toxic metals such as cadmium, lead, chromium, and mercury in water and wastewater.[18]

Besides MSPE, another widely used sample preparation method for determining metal ions is cloud point extraction (CPE). This is a physicochemical preconcentration technique based on the phase separation behavior of aqueous solutions of non-ionic surfactants when heated above the cloud point temperature. In this process, metal ions are first converted into hydrophobic species through complexation with suitable chelating agents and are then preferentially partitioned into the surfactant-rich phase, while the depleted aqueous phase is separated. The extraction efficiency is governed by hydrophobic interactions, partition equilibrium, metal-ligand complexation, and thermodynamic parameters of the system, such as temperature, pH, surfactant concentration, and ionic strength, leading to high preconcentration factors and reduced consumption of organic solvents.[25-27]

CPE is recognized for its simplicity, low cost, and minimal use of organic solvents, making it an eco-friendly option. Its use in trace metal analysis has been reported for elements such as cadmium, lead, copper, and nickel, often in combination with spectroanalytical methods to achieve low detection limits and high sensitivity.[26,40,41] However, despite these benefits, traditional CPE may still require extra steps such as centrifugation for phase separation and the use of complexing agents, which can reduce its operational simplicity. To offset these disadvantages, CPE has been combined with other extraction techniques, particularly ultrasound-induced solid-phase extraction,[42] which facilitates the interaction between the analyte, micelles, and the adsorbent.[43] Recent studies[43-45] have reported promising results in the extraction of metal ions and organic compounds from many types of samples, using a combination of CPE and other sample preparation techniques.

Considering the complementary strengths of both techniques, combining CPE and MSPE has become a promising alternative for trace metal analysis. MSPE is a sample preparation technique based on the use of magnetically sorbent materials to selectively isolate and/or preconcentrate analytes from complex matrices. In this approach, the analytes are adsorbed onto the surface of the magnetic sorbent through physical or chemical interactions, such as electrostatic attraction, coordination, or hydrophobic forces. After extraction, the sorbent is rapidly separated from the sample solution using an external magnetic field, eliminating the need for filtration or centrifugation.

The combination of CPE and MSPE offers significant analytical advantages over the use of each technique individually by integrating complementary extraction mechanisms within a single workflow. CPE provides efficient preconcentration based on the partitioning of hydrophobic metal-ligand complexes into a surfactant-rich phase, enabling high enrichment factors while minimizing the use of organic solvents. However, its performance can be limited by phase viscosity, incomplete phase separation, and potential surfactant interference during instrumental analysis. MSPE effectively addresses these limitations by introducing a selective adsorption step using magnetically responsive sorbents, which allows rapid isolation of analytes through an external magnetic field without the need for centrifugation or filtration. By integrating these methods, CPE-MSPE can overcome the

individual limitations of each approach, thereby enhancing selectivity, sensitivity, and operational efficiency in sample preparation.[46]

This study aims to develop a hybrid extraction method for detecting Cd^{II} in aqueous samples by combining CPE with MSPE using *Moringa oleifera* seed shells modified with magnetic fluids. The method seeks to merge the sustainability and low cost of a natural adsorbent with the convenience of magnetic separation and the preconcentration ability of micellar systems, offering an innovative and eco-friendly option for cadmium analysis in environmental samples.

Experimental

Materials and reagents

The working solutions were prepared with deionized water in a Millipore water purification system (Merck, Germany). The reagents were of analytical grade. Before use, the laboratory glassware was left overnight in an aqueous solution of 10% (v/v) nitric acid and then rinsed with deionized water. Working solutions of cadmium were prepared daily by diluting a 1000 mg L^{-1} standard solution (Carlo Erba, Val de Reuil, France). The nitric acid or sodium hydroxide solution used as eluant was prepared by diluting concentrated nitric acid obtained from Merck (Darmstadt, Germany) in water.

Instrumentation

Cadmium was detected using a Perkin Elmer AAnalyst 400 AA spectrometer (PerkinElmer) equipped with an air-acetylene flame, operating with a hollow cathode lamp at 228.80 nm, which was used for the detection of cadmium. The device was operated following the manufacturer's guidelines. The pH level of the samples and the working solutions was adjusted using a Hanna HI 2002, Edge® pH meter (São Paulo, Brazil). The solutions used in the extraction and elution steps were stirred in an XH-D vortex mixer (Global Trade Technology Co. Ltd., São Paulo, Brazil). The modified CPE procedure was performed using an Elmasonic E30H ultrasonic bath (Elmasonic) operating at 42 kHz and 100 W.

Methods

Synthesis of ferromagnetic fluid

This process involves adding an aqueous mixture of ferric chloride (40 mL, 1 mol L^{-1}) and ferrous chloride (10 mL of 2 mol L^{-1}, in 2 mol L^{-1} HCl) to an ammonia solution (500 mL, 0.7 mol L^{-1}). The gelatinous precipitate is isolated from the solution by centrifugation or magnetic decantation, without washing in water. After this, the precipitate is stirred with a two-molar aqueous perchloric acid solution and then isolated by centrifugation. Its peptization is accomplished merely by adding water.[47]

Magnetic modification of *M. oleifera* shells

Moringa oleifera seeds were collected in the city of Ituiutaba, Minas Gerais, Brazil. The shells were separated from the seeds and washed in ultrapure water from a Milli-Q water purification system (Millipore, Merck, Germany). They were then left to dry at room temperature, crushed in a domestic food blender, and sieved through an ordinary kitchen strainer.

After sieving, 3.00 g of *Moringa oleifera* shells were placed in a 40.0 mL beaker containing methanol and 6.0 mL of the previously prepared ferrofluid.[47-49] The mixture was stirred for one hour, then washed twice with methanol and dried at room temperature. The magnetic characteristics of the resulting materials were initially confirmed by applying an external magnetic field (magnet).

Characterization of magnetic adsorbent

The adsorbent thus obtained, was characterized using several techniques. The functional groups in the material were identified by infrared spectroscopy. Samples were prepared as potassium bromide tablets (KBr) with a 100:1 (KBr:sample) proportion and analyzed using a Shimadzu FTIR Prestige 21 Fourier transform infrared spectrophotometer (Tokyo, Japan). The samples were irradiated in the region of 4000-400 cm^{-1} at a resolution of 4 cm^{-1}. This procedure enabled the evaluation of natural and magnetized *M. oleifera* shells, revealing changes in the structure of the material and bonds after magnetic functionalization.

To analyze the pH_{PZC} of magnetized *M. oleifera*, aqueous solutions were prepared with pH levels varying from 2 to 11. 10.0 mL of each solution was placed separately in contact with 20.0 mg of adsorbent and left to rest for 24 h. The final pH of the solutions was then measured and plotted on a graph, showing the ΔpH levels as a function of the initial pH level.[30,50] This experiment was made in duplicate.

The morphology of magnetized shells was analyzed using scanning electron microscopy (SEM) in a Tescan VEGA 3 LMU microscope, coupled to an Oxford INCA X-ACT energy-dispersive spectrometer (EDS). Before this analysis, the samples were gold sputtered using a Quorum

QR 150ES sputter coater. X-ray diffraction (XRD) was used to elucidate the structure of the adsorbent and confirm the presence of magnetic material after functionalization. Three samples were analyzed: untreated *M. oleifera* shells, magnetized *M. oleifera* shells, and ferromagnetic fluid. The fluid was left to dry at room temperature before analysis.

MSPE combined with CPE

For the extraction procedure, 3.0 mg of the adsorbent were mixed into 10 mL of the sample solution, after which 2 mL of Triton X-100 solution were added. The mixture was then left in an ultrasonic bath for 10 min. After removing the mixture from the ultrasonic bath, it was heated in a water bath at 80 °C for 10 min and then cooled in an ice bath for 5 min. The cloud point formation was detected during this time.

The magnetic characteristics of the adsorbent used here allowed it to be separated from the liquid phase under a magnetic field. At this point, the metal ions had already been extracted, and the supernatant was discarded. A volume of 1.0 mL of the eluent was added to the solid phase, and the mixture was vortexed to trigger the desorption of the metal ions. The solid phase was then separated under a magnetic field, and the supernatant was analyzed by flame atomic absorption spectrometry (FAAS). The FAAS analysis was performed in a PerkinElmer AAnalyst 400 AA spectrometer equipped with an air-acetylene flame, operating with a hollow cathode lamp at 228.80 nm, which was used for the detection of cadmium.

Evaluation of pH level in the extraction process

The pH level of the medium is one of the main parameters that influences metal ion extraction processes. Thus, for the study of pH extraction, eight Cd^{II} solutions (1.0 mg L^{-1}) were prepared, and their pH levels were adjusted to a range of 4 to 11. Triton X-100 solution (3%) was used as surfactant, HNO_3 0.5 mol L^{-1} as eluent, and the water bath was set at 80 °C. Following the application of the modified CPE procedure, the supernatants, which had been eluted with nitric acid, were subjected to complete extraction, placed in an ice bath, and then underwent the adsorption process. FAAS subsequently analyzed them. This study was made in triplicate.

Evaluation of extraction conditions

A 2^4 factorial design (Table 1) with a central point was employed to study the influence of each variable of the modified CPE procedure, and their interactions. The pH extraction was adjusted at 6, and a Cd^{II} solution was prepared with a concentration of 1.0 mg L^{-1} and 3.0 mg of magnetic *M. oleifera* shells. All the experiments on factorial design were duplicated.

Table 1. Factorial design (2^4) matrix used for the evaluation of the steps of the modified CPE procedure

Run	Variable 1	Variable 2	Variable 3	Variable 4
	Triton-X 100 / %	Sonication time / min	Water bath heating / min	HNO_3 / (mol L^{-1})
1	1	1	1	0.1
2	5	1	1	0.1
3	1	10	1	0.1
4	5	10	1	0.1
5	1	1	10	0.1
6	5	1	10	0.1
7	1	10	10	0.1
8	5	10	10	0.1
9	1	1	1	1.0
10	5	1	1	1.0
11	1	10	1	1.0
12	5	10	1	1.0
13	1	1	10	1.0
14	5	1	10	1.0
15	1	10	10	1.0
16	5	10	10	1.0
17	3	5.5	5.5	0.55

After the results of factorial design were obtained, the sonication and heating times were evaluated individually. The sonication time was examined, after which the values of the other variables were set as follows: concentration of 1% Triton X-100, 10 min heating time in the water bath, and HNO_3 concentration of 1.0 mol L^{-1}. Sonication times were evaluated at 1, 2, 3, 5, 6, 8, 10, and 12 min.

Sonication time was set at 5 min, after which the heating time in the water bath was evaluated, repeating the procedure used for optimizing sonication time. The values of the other parameters were then set, with the heating time varying from 1 to 12 min. The adsorbent mass, another important parameter in analytical methods, was evaluated individually. Using the optimized parameters determined in the previous experiments, the amount of adsorbent mass varied from 2 to 20 mg.

Analytical performance of the method

Initially, the possible interfering ions were evaluated using a 2^{7-3} factorial design. Seven metal ions were chosen for this evaluation: Cu^{II}, Cr^{III}, Co^{II}, Pb^{II}, Fe^{III}, Mn^{II}, and

Ni^{II}. The Cd^{II} concentration was kept at 1 mg L^{-1} in all the experiments. The lowest level (–) fixed for the interfering ions was 0.0 mg L^{-1}, and the highest level (+) was 1.0 mg L^{-1}.

The stability of the adsorbent was evaluated by subjecting the same aliquot of 20.0 mg of adsorbent (magnetized *M. oleifera* shell) to 15 successive extractions using the CPE procedure in combination with SPE. The stability of the analytical signal recorded after the extraction and preconcentration procedure was evaluated.

The calibration curve was constructed from the analysis of standard solutions at increasing concentrations using the developed method. Each calibration point was analyzed in triplicate. The linearity of the resulting curve was evaluated by determining the coefficient of determination, performing residual analysis, and assessing the analytical sensitivity. The limit of detection (LOD) was estimated to be three times the standard deviation of ten independent measurements of a blank sample divided by the slope of the calibration curve. At the same time, the limit of quantification (LOQ) was 3.3 times this value, all obtained in accordance with International Union of Pure and Applied Chemistry (IUPAC) guidelines.[51]

To analyze repeatability, nine extractions were performed (1 mg L^{-1} of cadmium solution) at three different times on the same day-morning, afternoon, and evening. Conversely, to evaluate the intermediate precision of the method or reproducibility, nine extractions were carried out on three separate days under the same conditions described for the repeatability analysis.

The accuracy of the method was assessed through recovery tests using four different types of standard aqueous samples (mineral water, tap water, drinking water, and dam water). In this experiment, a calibration curve was created for each sample within the linear working range of the method.

Results and Discussion

Characterization of magnetized *Moringa oleifera* shell

Characterization of magnetized *M. oleifera* shells are a crucial step, enabling the detection of significant surface changes, particularly after the material has been magnetically functionalized. To verify the effectiveness of the magnetization process, the untreated material was subjected to an XRD analysis, as was the magnetized material, as well as the ferromagnetic fluid. Figure 1 depicts the XRD pattern of these materials.

The natural and magnetized *M. oleifera* shells showed peaks corresponding to the original structure, indicating

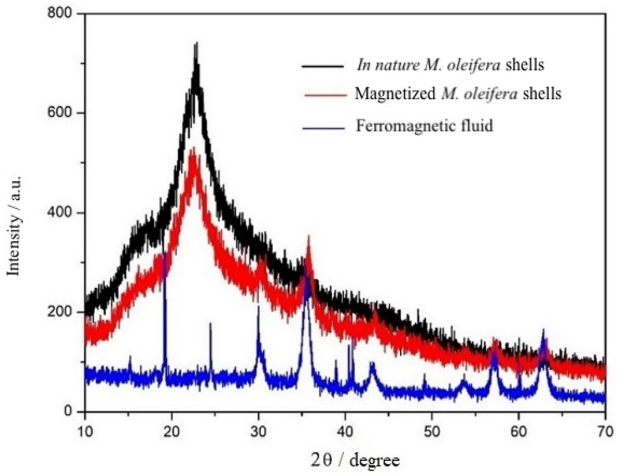

Figure 1. XRD patterns of the raw material and the material after the combined cloud-point extraction and solid-phase (CPE-MSPE) extraction procedures (Cu Kα radiation, λ = 1.5406 Å; 2θ = 5-80°).

that the main *M. oleifera* structure is preserved even after it has undergone magnetization. Moreover, no other peaks were observed in the untreated shells.

The diffractogram patterns of the other two materials, i.e., magnetized *M. oleifera* shells and ferromagnetic fluid, reveal a relationship between the spikes present in the fluid and those that appear on the magnetized *M. oleifera* shell, in the case of peaks corresponding to magnetite. This indicates that the magnetized *M. oleifera* seed shell contains a magnetite structure.

The FTIR analysis (Figure 2) revealed the absence of significant changes in the material after magnetic functionalization of *M. oleifera* shells, indicating that the functional groups contained in the structure of untreated *M. oleifera* shells, which are responsible for the adsorption process, are also present in the magnetized material. Note the characteristic O–H stretching bands of alcohols, phenols and water at around 3400 and 3000 cm^{-1}, stretching of symmetric and asymmetric vibrations of C–H bonds of hydrocarbons at around 2800 and 2900 cm^{-1}, and stretching bands at around 1600 cm^{-1} corresponding to C=O carbonyl and C–O ether bonds.[52] It is worth noting that the surface of the magnetized material contains Fe–O bonds, but these bonds normally appear in wavenumbers below 500 cm^{-1}, which is not clear in the infrared spectrum.

The SEM analysis (Figure 3) indicated that untreated *M. oleifera* shells have a heterogeneous matrix characteristic of amorphous and porous materials. However, a subsequent analysis of images of the magnetized material revealed an increase in pore size of the structure, possibly due to pore interconnectivity in the material prior to its magnetization.

Materials with large surface areas and high porosity are considered effective adsorbents.[53-55] Thus, an analysis of

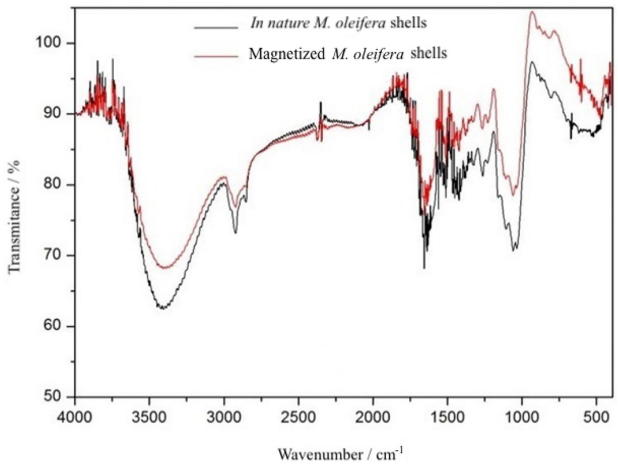

Figure 2. Infrared (KBr) spectra of the *in nature M. oleifera* seed and the magnetized material.

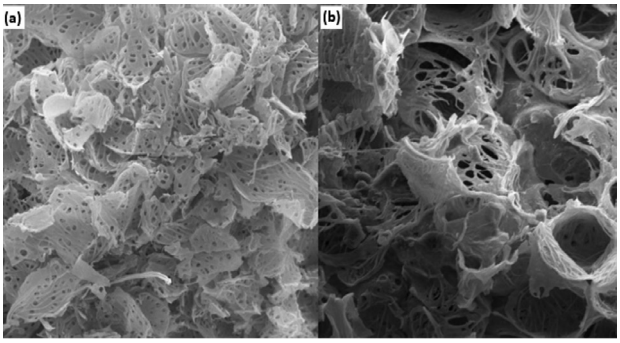

Figure 3. Micrographs of (a) natural *M. oleifera* and (b) magnetized *M. oleifera*, acquired at 1000 × magnification.

the presence of large numbers of pores and the functional groups in the magnetized *M. oleifera* seed shell, confirmed by FTIR, allows for the inference that the synthesized material will be an efficient adsorbent. The SEM-EDS analysis revealed the main chemical elements present in these materials. Before the *M. oleifera* shells underwent magnetization, the main elements they contained were carbon, oxygen, potassium, and sulfur, which are typically present in organic materials. However, since this is a comparative technique, the percentages of carbon and oxygen decreased after magnetization, while a significant percentage of iron was detected.

Determining the pH at the point of zero charge (pH_{PZC}) is essential for understanding the surface charge behavior of an adsorbent material and its influence on the adsorption of metal ions. Knowledge of the pH_{PZC} enables the optimization of solution pH, facilitates the interpretation of adsorption mechanisms, and supports the rational design of efficient adsorption processes for metal ion extraction. Figure 4 illustrates this behavior. At 6.4 pH, the surface charge of magnetized *M. oleifera* shells is neutral. Thus, when the magnetized *M. oleifera* shells were placed in a solution whose pH level exceeded that of pH_{PZC}, it was negative, preferentially favoring the adsorption of cations. In contrast, placing the adsorbent in a medium with a pH level below pH_{PZC} caused the predominant surface charge of the material to be positive, favoring anion adsorption.

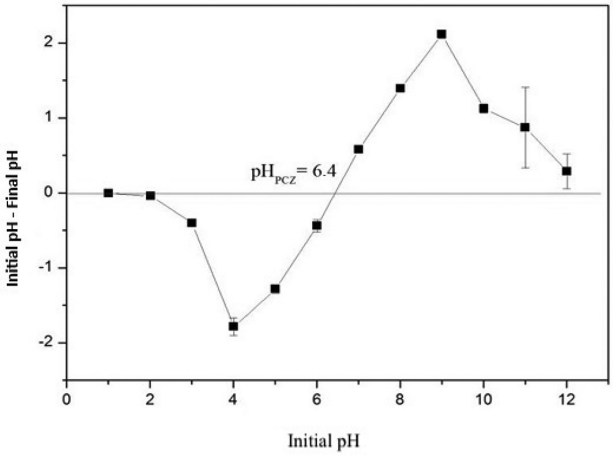

Figure 4. Determination of the point of zero charge (pH_{PZC}) of the magnetized *M. oleifera* shells using the ΔpH method. The pH_{PZC} corresponds to the pH at which the initial and final pH values intersect (ΔpH = 0), indicating the pH at which the surface has no net charge.

Evaluation of magnetic solid phase extraction combined with cloud point extraction

One of the most important variables in the extraction process is the pH level of the solution. Therefore, it is the first parameter to be studied separately, using pH levels that vary from more acidic (pH 4) to more basic (pH 11). Metal ion adsorption by an adsorbent is the result of a combination of physical and chemical interactions. The adsorption of an analyte onto adsorbent material may occur through physisorption or chemisorption. However, the latter involves the exchange or sharing of electrons between the analyte and the surface of the adsorbent, causing a chemical reaction that is stronger than that of physisorption. Figure 5 shows efficient adsorption over a wide range of pH levels, which is slightly higher at pH levels between 4 and 7. However, even at pH levels above 7, percentage adsorption exceeds 50%.

Given that the pH_{PZC} level is 6.4, pH levels above this one favor cation adsorption. Moreover, considering the species distribution of cadmium[56,57] in relation to pH medium, the species that prevails throughout the pH range is clearly the positive one Cd^{II}, which may explain the adsorption of this ion at pH levels above 7. The interaction of the metal ion with the surface of magnetized *M. oleifera* shells, where Fe–O bonds are present, can also occur through the formation of Lewis acid-base type bonds,

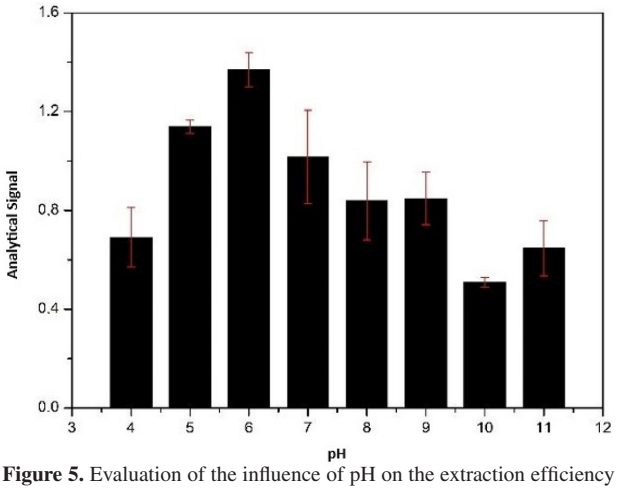

Figure 5. Evaluation of the influence of pH on the extraction efficiency of the proposed procedure (n = 3). The figure shows the variation in analytical response as a function of pH, indicating the optimal pH range for maximum extraction performance.

which may explain the percentage adsorption detected at pH levels lower than pH_{PZC}.

After establishing the pH level that enhances the adsorption process, other variables affecting the SPE combined with the CPE procedure were assessed using a 2^4 factorial design. These variables included the surfactant Triton X-100 concentration (% v/v), with a high (+) level of 5% and a low (–) level of 1%, and a midpoint at 3%. Two additional variables were sonication time and heating time in a water bath, with the maximum (+) at 10 min and the minimum (–) at 1 min, and a midpoint at 5.5 min. The final variable was the eluent concentration, specifically HNO_3, with a maximum (+) of 1.0 mol L^{-1}, a minimum (–) of 0.10 mol L^{-1}, and a midpoint at 0.55 mol L^{-1}.

Having completed the factorial planning, a Pareto chart was created (Figure 6) showing the effects of the main variables and their interactions at a 95% confidence level. The analysis of variance (ANOVA) table (Table S1, Supplementary Information (SI) section) indicates that 87% of the experimental data are explained by the chosen model. The chart also highlights two significant variables, namely sonication time and heating time. The effect of surfactant concentration shows a negative signal, indicating that this variable should be kept at its lowest level to maximize the analytical signal. Regarding eluent concentration, the analytical signal increases, suggesting that this variable has a positive effect and should be maintained at its highest level.

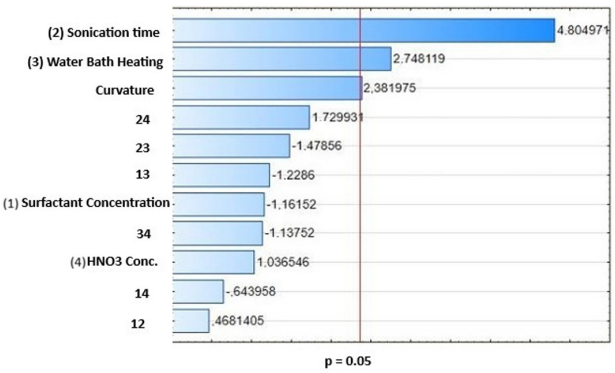

Figure 6. Pareto chart obtained from the factorial design used to evaluate the extraction variables for cadmium ions, highlighting the standardized effects of the investigated factors and their interactions, and enabling identification of the variables that significantly influence the extraction efficiency.

The concentration of Triton X-100 surfactant was set at 1% v/v, and the concentration of the eluent, HNO_3, was set at 1.0 mol L^{-1}.

A new experiment was conducted to provide a more detailed analysis of the variables that proved significant in the extraction process, and a univariate procedure was optimized. Since the variable with the greatest influence on the process was sonication time, this variable was examined first by fixing all other parameters and varying its duration from 1 to 12 min. The sonication times that produced the best values of the analytical signal were between 5 (approximately 1.0) and 10 min (approximately 0.9). However, considering the relative standard deviation (RSD) between the times of 5 and 10 min, the analytical signal appeared to be practically identical. Therefore, given the negligible difference in analytical signal and the analysis frequency, a sonication time of 5 min was selected for future experiments.

After optimizing the sonication time, the effect of heating time in a water bath was assessed. At a heating time of less than 5 min, the analytical signal was lower than at longer times, although a roughly 4.5-fold preconcentration was already detectable. However, for improved extractions and subsequent preconcentration, the 6-min heating time proved to be the most effective and was therefore chosen as the standard.

Another important parameter in SPE methods is the adsorbent mass. This parameter was also analyzed using a univariate approach, which showed that increasing the mass results in a corresponding rise in absorbance. This observation led to using a larger amount of adsorbent to ensure optimal adsorption and effective extraction of Cd^{II}. Using adsorbent masses larger than 20.0 mg did not significantly boost the analytical signal, indicating that smaller amounts are more effective for extraction. Additionally, practically speaking, separating the adsorbent from the solution becomes more difficult and hampers both adsorption and desorption when using more than 20.0 mg. Therefore, the rest of the experiments were carried out with an adsorbent mass of 20.0 mg.

Evaluation of the proposed procedure and analytical performance

Most studies in the literature that report using a combination of two techniques apply one technique followed by the other, e.g., when the rich phase is subjected to solid-phase extraction, or the solid phase is subjected to cloud-point extraction. In this regard, to illustrate the efficiency of the proposed method, Figure 7 depicts the analytical signals obtained for a cadmium solution subject to five different extraction processes, using the optimized conditions: (*i*) solely SPE using magnetized *M. oleifera* shells, (*ii*) this work, (*iii*) SPE followed by CPE, (*iv*) CPE followed by SPE, (*v*) solely CPE.

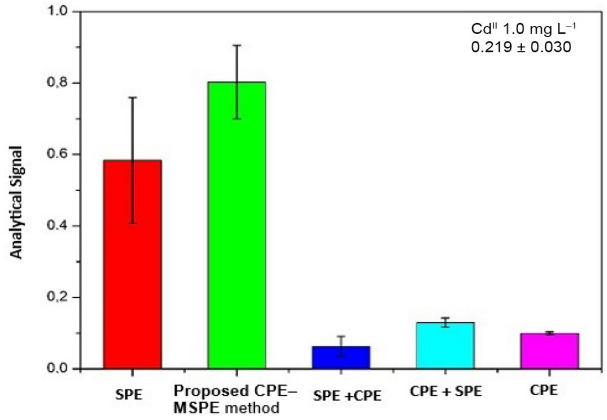

Figure 7. Comparison of the different extraction arrangements evaluated for the simultaneous application of the two procedures investigated in this study (n = 3): (*i*) SPE using only magnetized *M. oleifera* shells; (*ii*) proposed combined procedure (this study); (*iii*) SPE followed by CPE; (*iv*) CPE followed by SPE; and (*v*) CPE only. SPE: solid-phase extraction; CPE-MSPE: magnetic solid-phase extraction cloud point extraction; CPE-SPE: cloud point extraction solid-phase extraction; SPE-CPE: solid-phase extraction cloud point extraction; CPE: cloud point extraction.

Figure 7 clearly shows that the analytical signal increases when the extraction procedure is performed concomitantly. Several analytical characteristics of the proposed method were evaluated after the system was optimized.

Calibration curves for chromium were established using blank and aqueous standard solutions. The calibration equation was A = 0.0018C + 0.0080, where A is the absorbance signal and C is the concentration of cadmium in μL^{-1}. The linear regression coefficient, LOD, and LOQ were 0.9998, 3.45 $\mu g\ L^{-1}$, and 11.5 $\mu g\ L^{-1}$, respectively, all determined in accordance with the guidelines of the International Union of Pure and Applied Chemistry (IUPAC).[51] The relative standard deviation (RSD) for the replicates was estimated at 7.71%. The enhancement factor was calculated as the ratio between the slope of a calibration curve obtained after preconcentration using the combined procedure and the slope of a calibration curve without preconcentration. An enrichment factor of 4 was achieved through preconcentration during the extraction process. The low preconcentration factor observed for the combined method can be attributed to physicochemical and operational factors, particularly the high viscosity of the surfactant-rich phase, which limits mass transfer and reduces adsorption efficiency during the MSPE step. In addition, increased ionic strength may interfere with metal ion-sorbent interactions, compromising analyte retention. Losses occurring during phase separation or desorption steps may further contribute to the reduced preconcentration factor.

The proposed method was used to detect cadmium in samples of river, tap, and mineral water. The samples were fortified with 50.0 μL^{-1} Cd solution. The results are shown in Table 2. Before analysis, the pH levels of the samples were adjusted to 6. Cadmium recovery test results confirm the absence of matrix effects, as the values obtained fall within the acceptable range of 95 to 115%.[30]

Another important characteristic of the evaluated method is selectivity. The selectivity of the analytical method can be defined by its ability to identify or quantify the analyte, even in the presence of components that may be present in the sample or its matrix.

For this study, a 2^{7-3} fractional factorial design was used, leading to a total of 16 experiments (Table 3). In Figure 8, it is observed that the metal ion with the most significant effect is lead, followed by copper and then cobalt. The higher interference factors observed for these ions can be mechanistically attributed to their high charge density

Table 2. Recoveries obtained for the proposed method at three concentration levels (n = 3), demonstrating its accuracy and applicability across the evaluated range

Sample	Add 50 $\mu g\ L^{-1}$ Cd^{II}		Add 250 $\mu g\ L^{-1}$ Cd^{II}		Add 250 $\mu g\ L^{-1}$ Cd^{II}	
	Found / ($\mu g\ L^{-1}$)	Recovery / %	Found / ($\mu g\ L^{-1}$)	Recovery / %	Found / ($\mu g\ L^{-1}$)	Recovery / %
1	56.89 ± 0.09	113.78	293.56 ± 0.06	117.42	105.33 ± 0.16	105.13
2	52.33 ± 0.04	104.67	281.50 ± 0.07	112.60	984.83 ± 0.04	98.48
3	53.27 ± 0.08	106.53	241.93 ± 0.03	96.77	1140.60 ± 0.04	114.06
4	40.20 ± 0.04	80.40	214.87 ± 0.05	85.95	950.20 ± 0.06	95.02

and similar coordination chemistry, which promote strong interactions with the active sites of the magnetic sorbent. At solution pH values above the point of zero charge (pH_{PZC}) of the adsorbent, the negatively charged surface enhances electrostatic attraction toward these cations, intensifying competitive adsorption and reducing the selectivity for Cd^{II} during the MSPE step.

Other types of interference can occur not only during the competition for active sites during adsorption but also in the final step of the analysis, which is atomization in the FAAS instrument. Interference during atomization happens when an easily ionizable element affects the ionization of a less ionizable element. Specifically, elements that ionize easily produce electrons that shift the ionization equilibrium of the analyte, promoting the formation of neutral atoms.[58]

However, since these ions were studied at concentrations above trace level (concentrations below ppb), this interference does not represent a problem for this newly developed analytical method.

The stability of magnetized *M. oleifera* shells was evaluated through successive extraction cycles, based on the optimized parameters, using the adsorbent portion. The results indicate that the proposed adsorbent has low stability, preventing its reuse in other extractions. This low stability can be mainly attributed to the elution step, in which exposure to acidic media promotes partial leaching of the magnetic phase from the natural support. This process reduces both magnetization and the availability of active adsorption sites, leading to decreased adsorption capacity and overall extraction efficiency.

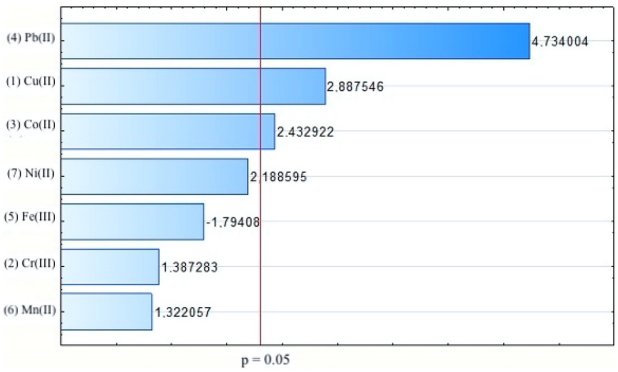

Figure 8. Pareto chart derived from the factorial design matrix, showing the standardized effects of the investigated metal ions and their interactions on the analytical response.

However, the low stability of the adsorbent does not interfere with the extraction of the metal ion. Additionally, it is a low-cost material, making it advantageous over other methods that use synthetic and more expensive adsorbents.

The analytical performance of the developed CPE-MSPE method was compared with similar studies for the metal ion determination in a variety of samples (Table 4). The comparative analysis presented emphasizes some analytical parameters of each approach rather than a full analytical validation dataset.

Conclusions

The proposed CPE-MSPE methodology offers significant analytical and environmental advantages compared to conventional FAAS-based preconcentration

Table 3. Fractional factorial design matrix and corresponding analytical absorbance responses used for the multivariate evaluation of the effects of interfering ions

Run	Cu^{II} / (mg L^{-1})	Cr^{III} / (mg L^{-1})	Co^{II} / (mg L^{-1})	Pb^{II} / (mg L^{-1})	Fe^{III} / (mg L^{-1})	Mn^{II} / (mg L^{-1})	Ni^{II} / (mg L^{-1})	Analytical signal
1	0.0	0.0	0.0	0.0	0.0	0.0	0.0	0.402
2	1.0	0.0	0.0	0.0	1.0	0.0	1.0	0.463
3	0.0	1.0	0.0	0.0	1.0	1.0	0.0	0.461
4	1.0	1.0	0.0	0.0	1.0	1.0	1.0	0.495
5	0.0	0.0	1.0	0.0	0.0	1.0	1.0	0.507
6	1.0	0.0	1.0	0.0	0.0	1.0	0.0	0.534
7	0.0	1.0	1.0	0.0	1.0	0.0	1.0	0.492
8	1.0	1.0	1.0	0.0	0.0	0.0	0.0	0.514
9	0.0	0.0	0.0	1.0	1.0	1.0	1.0	0.488
10	1.0	0.0	0.0	1.0	1.0	1.0	0.0	0.546
11	0.0	1.0	0.0	1.0	0.0	0.0	1.0	0.570
12	1.0	1.0	0.0	1.0	0.0	0.0	0.0	0.523
13	0.0	0.0	1.0	1.0	0.0	0.0	0.0	0.528
14	1.0	0.0	1.0	1.0	0.0	0.0	1.0	0.597
15	0.0	1.0	1.0	1.0	1.0	1.0	0.0	0.514
16	1.0	1.0	1.0	1.0	1.0	1.0	1.0	0.584

Table 4. Comparison of the analytical performance of the CPE-MSPE analytical method with studies published previously on the metal ion determination

Method	Analyte	LOD / (μg L^{-1})	LOQ / (μg L^{-1})	Preconcentration factor	Sample	Detection	Reference
CPE-MSPE	Cd^{II}	0.45	11.5	4	aqueous	FAAS	this work
UA-CPE	Co^{II}	0.76	2.59	N.I	spices	FAAS	59
UA-CPE + D-μSPE	Cd^{II}	0.08	0.27	150	aqueous	ICP-OES	42
CPE	Mo^{VI}	1.5	5.0	11.5	water and pea	UV-Vis	60
CPE-MSPE	Cr^{III}	3.2	10.5	12	biological samples	FAAS	46
MSPE	Pb^{II}	5.44	16.48	135	water	FAAS	61

CPE-MSPE: magnetic solid-phase extraction cloud point extraction; UA-CPE: ultrasound assisted cloud point extraction; UA-CPE + D-μSPE: ultrasound assisted cloud point extraction and dispersive μ-solid phase extraction; CPE: cloud point extraction; MSPE: magnetic solid-phase extraction; N.I: not informed; FAAS: flame atomic absorption spectrometry; ICP-OES: inductively coupled plasma optical emission spectrometry; UV-Vis: ultraviolet-visible spectrophotometry; LOD: limit of detection; LOQ: limit of quantification.

approaches. The method provides adequate sensitivity for cadmium determination using simple pH control as the only sample pretreatment step, reducing operational complexity. The use of magnetized *M. oleifera* shells as a low-cost, easily available, and renewable sorbent aligns the method with Green Analytical Chemistry principles by minimizing reagent consumption and waste generation. In addition, satisfactory accuracy and recovery demonstrate the reliability of the method, while its simplicity and cost-effectiveness make it a competitive alternative to more complex FAAS preconcentration strategies reported in the literature.

Supplementary Information

Supplementary information is available free of charge at http://jbcs.sbq.org.br as PDF file.

Data Availability Statement

All data are available in the text.

Acknowledgments

The authors gratefully acknowledge the financial support provided by CAPES (financing code 001), CNPq, FAPEG. We also thank Universidade Federal de Catalão (UFCAT) for providing research infrastructure.

Author Contributions

D. C. B. G., J. M. S., W. R. S., V. N. A.: conceptualization; D. C. B. G., J. M. S., W. R. S.: methodology, writing original draft; D. C. B. G.: investigation; V. N. A.: project administration, resources, writing (review and editing).

References

1. Ogwu, M. C.; Izah, S. C.; Sawyer, W. E.; Amabie, T.; *Environ. Geochem. Health* **2025**, *47*, 94. [Crossref]
2. Li, Z.; Zhang, W.; Wang, S.; Jiang, X.; Guo, H.; Liu, Y.; Fu, Z.; *Processes* **2025**, *13*, 2140. [Crossref]
3. Akmal, N.; Faez, M.; Jalal, A.; Chowdhury, K.; Hafizah, N.; *Desalin. Water Treat.* **2023**, *294*, 79. [Crossref]
4. Zhang, P.; Yang, M.; Lan, J.; Huang, Y.; Zhang, J.; Huang, S.; Yang, Y.; Ru, J.; *Toxics* **2023**, *11*, 828. [Crossref]
5. Singh, V.; Singh, N.; Rai, S. N.; Kumar, A.; Singh, A. K.; Singh, M. P.; Sahoo, A.; Shekhar, S.; Vamanu, E.; Mishra, V.; *Toxics* **2023**, *11*, 147. [Crossref]
6. Manwani, S.; Devi, P.; Singh, T.; Yadav, C. S.; Awasthi, K. K.; Bhoot, N.; Awasthi, G.; *Environ. Sci. Pollut. Res.* **2023**, *30*, 71940. [Crossref]
7. Filipoiu, D. C.; Bungau, S. G.; Endres, L.; Negru, P. A.; Bungau, A. F.; Pasca, B.; Radu, A. F.; Tarce, A. G.; Bogdan, M. A.; Behl, T.; Nechifor, A. C.; Hassan, S. S. ul; Tit, D. M.; *Toxics* **2022**, *10*, 716. [Crossref]
8. Das, S.; Sultana, K. W.; Ndhlala, A. R.; Mondal, M.; Chandra, I.; *Environ. Health Insights* **2023**, *17*, 1. [Crossref]
9. Sahu, P.; Patel, A. R.; Pandey, A.; Hait, M.; Patra, G. K.; *Inorg. Chim. Acta* **2025**, *585*, 122751. [Crossref]
10. Pan, Z.; Gong, T.; Liang, P.; *Circ. Res.* **2024**, *134*, 1160. [Crossref]
11. Morelli, E.; Scarano, G.; *Chem. Speciation Bioavailability* **1995**, *7*, 43. [Crossref]
12. Kubier, A.; Wilkin, R. T.; Pichler, T.; *Appl. Geochem.* **2019**, *108*, 104338. [Crossref]
13. Turner, A.; *Sci. Total Environ.* **2019**, *657*, 1409. [Crossref]
14. Radwan, A.; El-Sewify, I. M.; Azzazy, H. M. E. S.; *ACS Omega* **2022**, *18*, 15739. [Crossref]
15. Jomova, K.; Alomar, S. Y.; Nepovimova, E.; Kuca, K.; Valko, M.; *Heavy Metals: Toxicity and Human Health Effects*; Springer: Berlin, 2025.

16. Iyer, S.; Deshmukh, S. M.; Tapre, R. W.; *Rev. Inorg. Chem.* **2024**, *45*, 479. [Crossref]
17. Inobeme, A.; Mathew, J. T.; Jatto, E.; Inobeme, J.; Adetunji, C. O.; Muniratu, M.; Onyeachu, B. I.; Adekoya, M. A.; Ajai, A. I.; Mann, A.; Olori, E.; Akhor, S. O.; Eziukwu, C. A.; Kelani, T.; Omali, P. I.; *Environ. Monit. Assess.* **2023**, *195*, 452. [Crossref]
18. Pasupuleti, R. R.; Huang, Y. L.; *J. Chin. Chem. Soc.* **2023**, *70*, 1326. [Crossref]
19. Korkmaz, Ş.; Kurnaz Yetim, N.; Koç, M. M.; Özcan, C.; *Chem. Pap.* **2024**, *78*, 4495. [Crossref]
20. Leal, G. C.; Rovasi, F.; Maziero, M.; do Nascimento, P. C.; de Carvalho, L. M.; Viana, C.; *J. Food Compos. Anal.* **2022**, *112*, 104651. [Crossref]
21. de Souza, R. M.; Toloza, C. A. T.; Aucélio, R. Q.; *J. Trace Elem. Miner.* **2022**, *2*, 100011. [Crossref]
22. Mdluli, N. S.; Knottenbelt, C. D.; Nomngongo, P. N.; Mketo, N.; *Sci. Rep.* **2024**, *14*, 2362. [Crossref]
23. Nomngongo, P. N.; Ngila, J. C.; *Spectrochim. Acta, Part B* **2014**, *98*, 54. [Crossref]
24. Lindenmayer, R.; Lu, L.; Eivazi, F.; Afrasiabi, Z.; *Appl. Sci.* **2023**, *13*, 4764. [Crossref]
25. Poojary, H.; Selvamuthukumar, K.; Parveen, R.; Illanad, G.; Mandal, D.; Koo, S.; Ghosh, C.; *Green Chem. Lett. Rev.* **2025**, *18*, 2486135. [Crossref]
26. Sznek, B.; Kupczyk, O.; Czyrski, A.; *Processes* **2025**, *13*, 430. [Crossref]
27. Viana, J. L. M.; Menegário, A. A.; Fostier, A. H.; *Talanta* **2021**, *226*, 122119. [Crossref]
28. Paniagua, C. E. S.; Costa, B. E. S.; Alves, V. N.; Coelho, N. M. M.; *Rev. Virtual Quim.* **2021**, *13*, 551. [Crossref]
29. Neto, J. A. D. S.; Oliveira, J. D. A. N.; Siqueira, L. M. C.; Alves, V. N.; *J. Chem.* **2019**, *2019*, 1. [Crossref]
30. Silva, W.; Costa, B.; Batista, A.; Alves, V.; Coelho, N.; *J. Braz. Chem. Soc.* **2022**, *33*, 498. [Crossref]
31. Alves, V. N.; Mosquetta, R.; Carasek, E.; Coelho, N. M. M.; *J. Anal. Chem.* **2012**, *67*, 448. [Crossref]
32. Alves, V. N.; Mosquetta, R.; Coelho, N. M. M.; Bianchin, J. N.; Roux, K. C. P.; Martendal, E.; Carasek, E.; *Talanta* **2010**, *80*, 1133. [Crossref]
33. Ju, S.; Liu, M.; Yang, Y.; *Anal. Lett.* **2016**, *49*, 511. [Crossref]
34. Simões, A. R.; Souza, A. T. de; Meurer, E. C.; Scaliante, M. H. N. O.; Cortelo, T. H.; *Cad. Pedagógico* **2025**, *22*, e13594. [Crossref]
35. Dias, F. D. S.; Meira, L. A.; Carneiro, C. N.; Lucas, F. M.; Coelho, N. M. M.; Coelho, L. M.; Alves, V. N.; Guimar, L. B.; *TrAC, Trends Anal. Chem.* **2023**, *158*, 116891. [Crossref]
36. Öztürk Er, E.; Dalgıç Bozyiğit, G.; Büyükpınar, Ç.; Bakırdere, S.; *Crit. Rev. Anal. Chem.* **2022**, *52*, 231. [Crossref]
37. Silva, A. K.; Sobieski, E.; Viana, L. H.; Lanças, F. M.; Nazario, C. E. D.; *Sci. Chromatogr.* **2016**, *8*, 239. [Crossref]
38. Ricardo, A. I. C.; Abujaber, F. F.; Bernardo, J. G.; Martín-Doimeadios, R. C. R.; Ríos, A.; *Trends Environ. Anal. Chem.* **2020**, *27*, e00097. [Crossref]
39. Moral, A.; Borrull, F.; Marcé, R. M.; Fontanals, N.; *TrAC, Trends Anal. Chem.* **2024**, *181*, 118005. [Crossref]
40. Abdelwahed, F. T.; Mortada, W. I.; El-Defrawy, M. M.; Eltabey, R. M.; *J. Food Compos. Anal.* **2024**, *129*, 106119. [Crossref]
41. Thuy, T. T. T.; Phong, H. T.; Van Trong, N.; Van Dat, D.; *Vietnam J. Chem.* **2022**, *60*, 451. [Crossref]
42. Nyaba, L.; Nomngongo, P. N.; *Food Chem.* **2020**, *322*, 126749. [Crossref]
43. Biata, N. R.; Mashile, G. P.; Ramontja, J.; Mketo, N.; Nomngongo, P. N.; *J. Food Compos. Anal.* **2019**, *76*, 14. [Crossref]
44. Pourreza, N.; Naghdi, T.; *Talanta* **2014**, *128*, 164. [Crossref]
45. Mahmoodnezhad, D.; Taheri, A.; *J. Food Compos. Anal.* **2022**, *111*, 104594. [Crossref]
46. Diniz, K. M.; Tarley, C. R. T.; *Microchem. J.* **2015**, *123*, 185. [Crossref]
47. Massart, R.; *IEEE Trans. Magn.* **1981**, *17*, 1247. [Crossref]
48. Alizadeh, M.; Peighambardoust, S. J.; Foroutan, R.; Azimi, H.; Ramavandi, B.; *Environ. Res.* **2022**, *212*, 113242. [Crossref]
49. Milonjic, S. K.; Ruvarac, A. L.; Šušić, M. V.; *Thermochim. Acta* **1975**, *11*, 261. [Crossref]
50. Khan, M. N.; Sarwar, A.; *Surf. Rev. Lett.* **2007**, *14*, 461. [Crossref]
51. Vessman, J.; Stefan, R. I.; van Staden, J. F.; Danzer, K.; Lindner, W.; Burns, D. T.; Fajgelj, A.; Müller, H.; *Pure Appl. Chem.* **2001**, *73*, 1381. [Crossref]
52. Socrates, G.; *Infrared and Raman Characteristic Group Frequencies*, 3rd ed.; John Wiley & Sons: Chichester, 2001.
53. Wuana, R. A.; Sha'Ato, R.; Iorhen, S.; *Desalin. Water Treat.* **2016**, *57*, 11904. [Crossref]
54. Oladele, I. O.; Ogunwande, G. S.; Taiwo, A. S.; Lephuthing, S. S.; *Heliyon* **2022**, *8*, e09755. [Crossref]
55. de Olivera, A.; Kreutz, C.; Martins, R.; *Acad. Soc. J.* **2020**, 99. [Crossref]
56. Nahar, N.; Ramim, A.; Abser, M. N.; *Bangladesh J. Sci. Ind. Res.* **1970**, *44*, 1. [Crossref]
57. Rodríquez-Serrano, M.; de la Casa, N. M.; Romero-Puertas, M. C.; del Río, L. A.; Sandalio, L. M.; *Ecosistemas* **2008**, *17*, 139. [Crossref]
58. Skoog, D. A.; West, D. M.; Holler, F. J.; *Fundamentals of Analytical Chemistry*, 8th ed.; Thomson: São Paulo, 2006.
59. Temel, N. K.; Çöpür, M.; *J. Mol. Struct.* **2023**, *1284*, 135433. [Crossref]
60. Snihur, K.; Zhukovetska, O.; Al-Muhanna, E. A.; Guzenko, O.; Azooz, E. A.; Snigur, D.; *Talanta* **2026**, *298*, 129011. [Crossref]
61. Silva, C. A. S.; Silva, R. L. S.; Figueiredo, A. T.; Alves, V. N.; *J. Braz. Chem. Soc.* **2020**, *31*, 109. [Crossref]

Submitted: December 10, 2025
Final version online: March 24, 2026